

Electronic Supplementary Information

Molecular Dynamics study of the dynamics of [EMIM][TFSI]/(Li/Na)TFSI ionic liquids confined in silica pores

Samanvitha Kunigal Vijaya Shankar¹, Chris Ewels¹, Jean Le Bideau¹, and Yann Claveau^{1,*}

¹Nantes Université, CNRS, Institut des Matériaux de Nantes Jean Rouxel, IMN, F-44000 Nantes, France

*yann.claveau@cnrns-imn.fr

1 Density convergence of Neat [EMIM][TFSI] ionic liquid

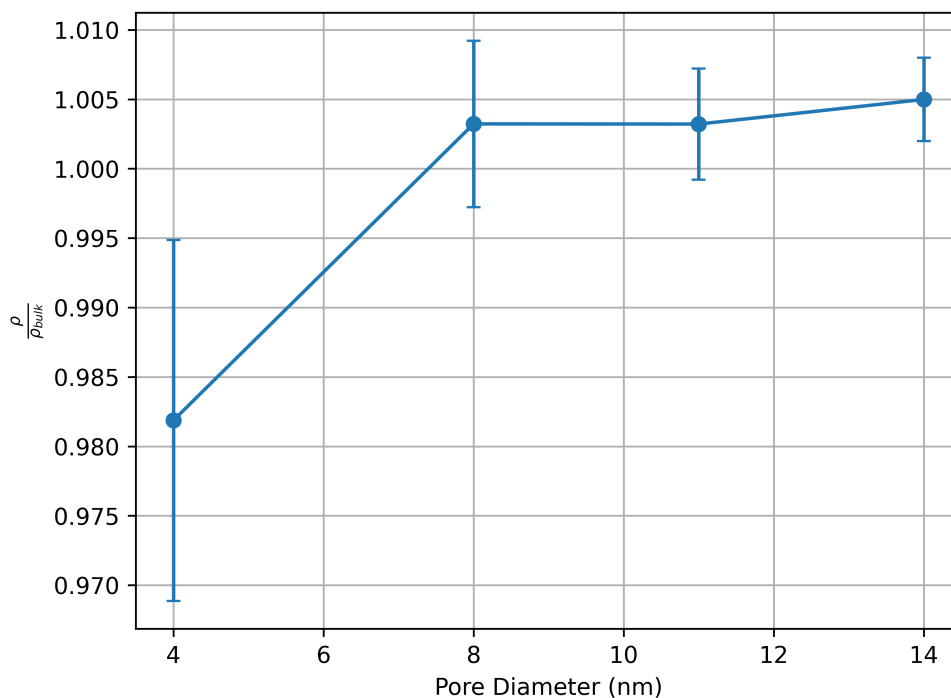


Figure S1 Density of confined neat [EMIM][TFSI] ionic liquid obtained through NPAV_zT method at 393 K for different pore diameters ranging from 4 nm to 14 nm. The experimental density of non-confined ionic liquid is obtained by extrapolating the density data from Tokuda *et.al*¹ for 393 K

2 Dimensions of simulation boxes

Pore diameter (nm)	Simulation box dimensions (x × y × z) (nm)
4	7.26 × 7.26 × 7.26
8	10.69 × 10.69 × 7.26
11	14.26 × 14.26 × 7.26
14	17.83 × 17.83 × 7.26

Table S1 Dimensions of simulation box in nm

3 Composition of the systems

Diameter (nm)	Radius (nm)	Concentration	Density (g/cm ³)	n_{EMIM}	n_{TFSI}	$n_{metalcation}$
4	2.0	0.04	1.442	192	200	8
		0.12	1.466	184	208	24
		0.24	1.509	168	222	54
8	4.0	0.24	1.509	674	886	212
11	5.5	0.24	1.509	1274	1676	402
14	7.0	0.24	1.509	2064	2716	652

Table S2 Density and composition of the systems at different concentrations and pore sizes

4 Equilibration and production simulation times

Pore diameter (nm)	Time (ns)
4	5
8	10
11	20
14	25

Table S3 Equilibration time lengths (in ns) for all metal cation systems at 0.24 concentration

System/Pore diameter (nm)	4	8	11	14
Li system	125	135	100	50
Na system	125	100	120	50

Table S4 Production time lengths (in ns) for all metal cation systems at 0.24 concentration

System/Concentration	0.04	0.12	0.24
Li system	100	115	125
Na system	95	110	125

Table S5 Production lengths (in ns) for all the metal cation systems at different concentration for 4nm pore

5 Mass density profiles

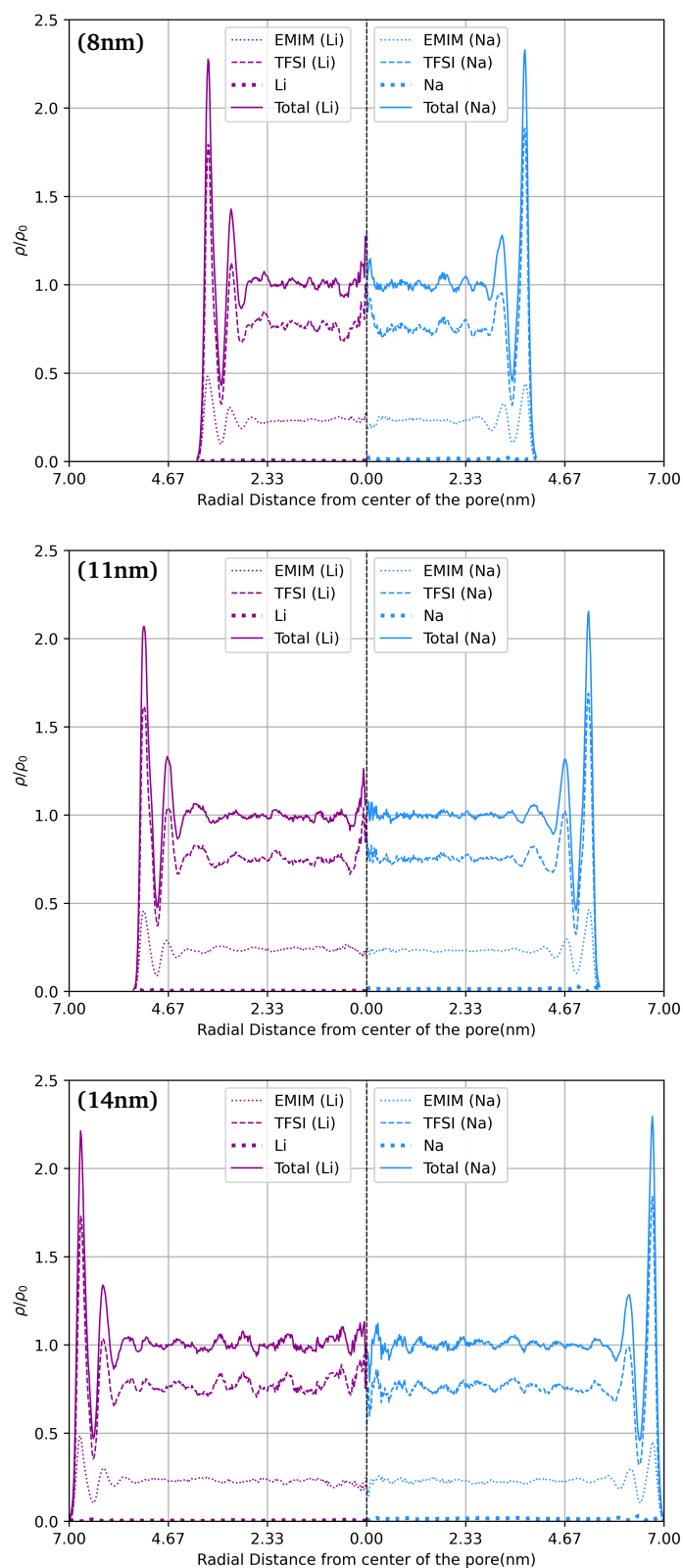
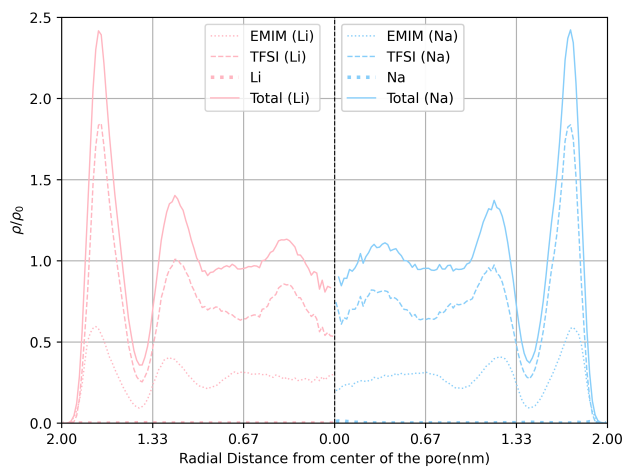
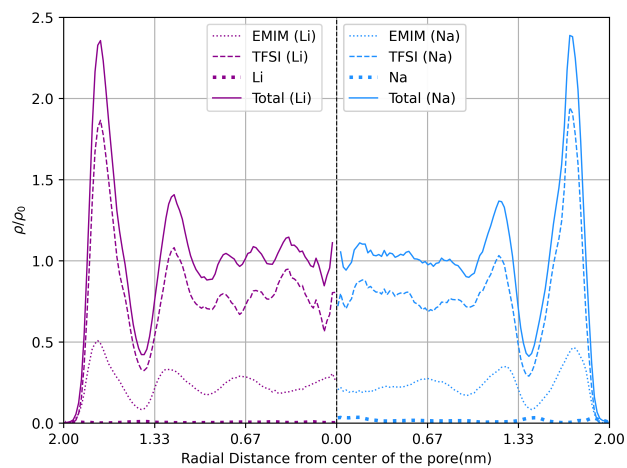


Figure S2 Radial mass density profiles depicted in increasing order of pore diameter from 8 nm (top) to 14 nm (bottom) at 0.24 concentration of metal cation. Pink and blue shades represent ions in Li (left) systems and Na (right) systems respectively. Solid lines represent the total contribution of all the species to density profiles, dotted lines correspond to EMIM ions, dashed lines correspond to TFSI ions and spaced squares correspond to metal cations.



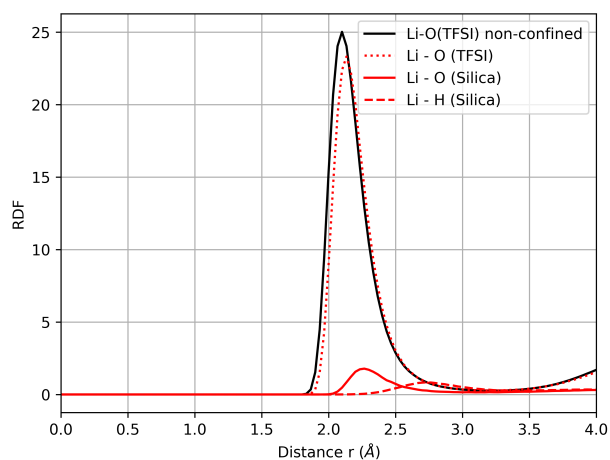
(a) 0.04



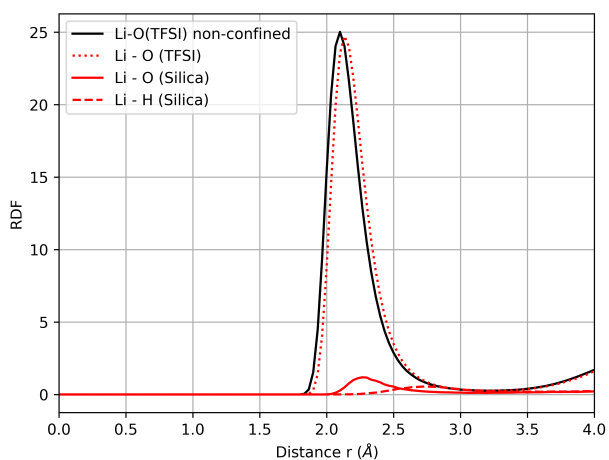
(b) 0.24

Figure S3 Mass density profiles for Li/Na systems confined inside a silica pore of 4nm diameter at different concentrations.

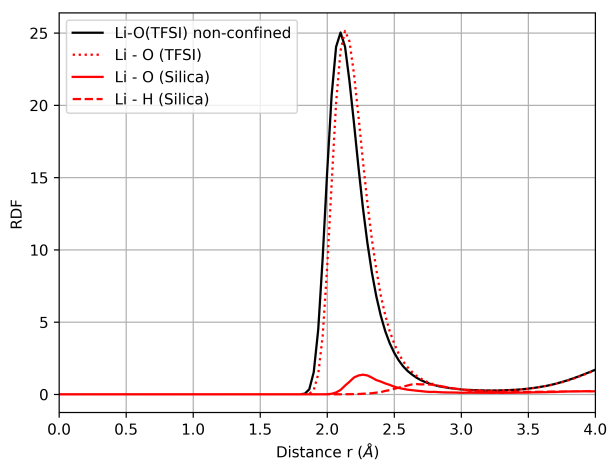
6 Radial distribution functions



(a) 4nm

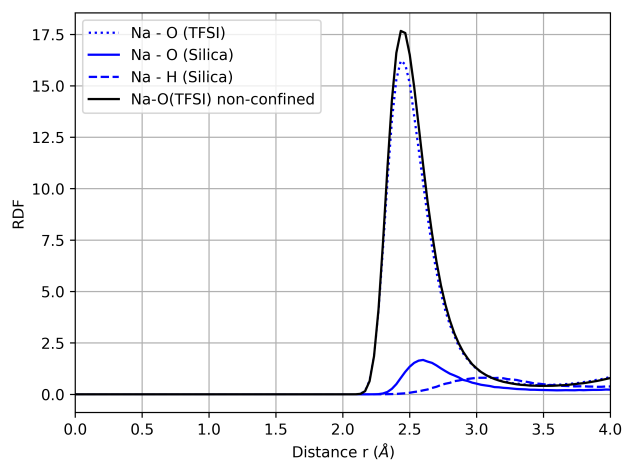


(b) 8 nm

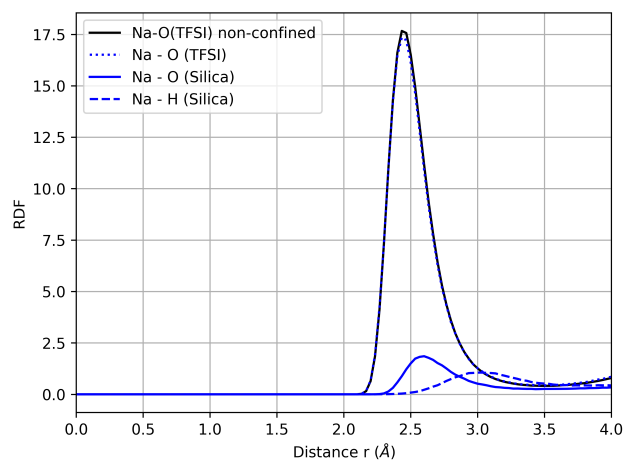


(c) 14nm

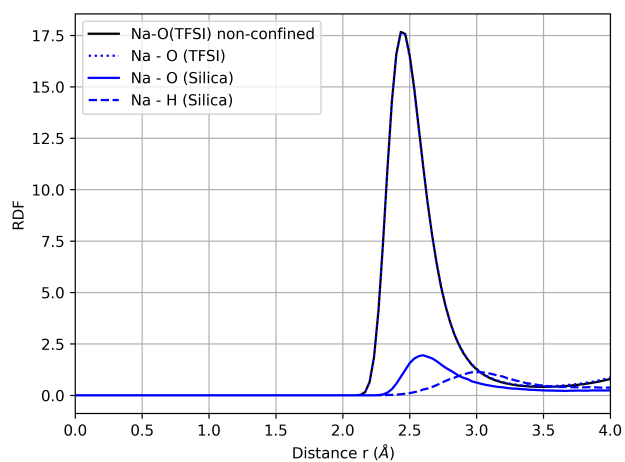
Figure S4 Radial distribution functions for Li⁺ systems at different pore diameters: (a) 4 nm, (b) 8 nm and (c) 14 nm



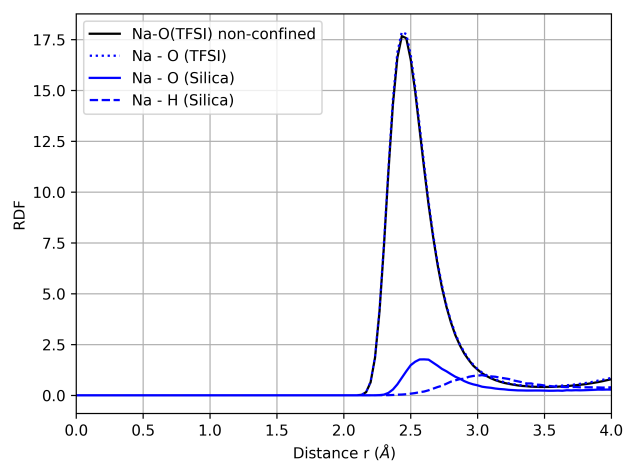
(a) 4 nm



(b) 8 nm



(c) 11 nm



(d) 14 nm

Figure S5 Radial distribution functions of Na⁺ systems at different pore sizes: (a) 4 nm, (b) 8 nm, (c) 11 nm, and (d) 14 nm.

7 Methodology to calculate region-wise diffusion coefficients

The methodology for studying the diffusion of ions in the centre and interface region is taken from Gäding *et al.*² and adapted to cylindrical pores. As depicted in radial density profiles, the pore is divided into two regions, i.e. the centre (away from the pore wall) and interface (close to the pore). The radius of the interface region is 11 Å, while the centre radius is calculated as $(r - 11)$ Å, with r being the radius of the pore. Ions contribute to the MSD of a given region as long as they reside in that region. When an ion enters a new region, its contribution to the MSD in the previous region is terminated, and its contribution in the new region begins, as depicted in Fig. S6.

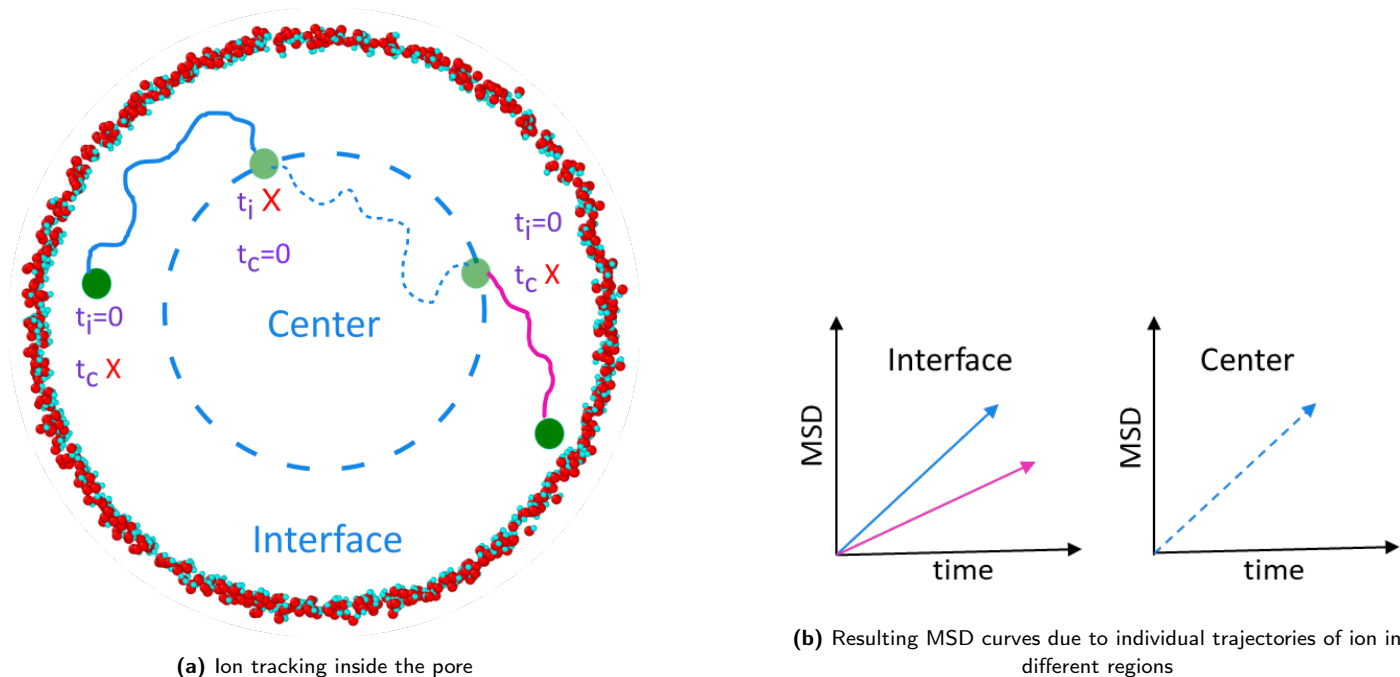


Figure S6 Schematics for region-wise MSD calculation in cylindrical pore. The pore is divided into two regions i.e. centre and interface. The t_i and t_c in (a) denote the starting times of the ion in the centre and interface regions, respectively.

A window algorithm is implemented in the analysis to minimise the noise in the resulting MSD curves. Curve fitting was carried out by excluding the initial 2 nanoseconds in the linear regime of the MSD curves. The corresponding code executed in Dynopore package can be found in our lab's Gitlab.³

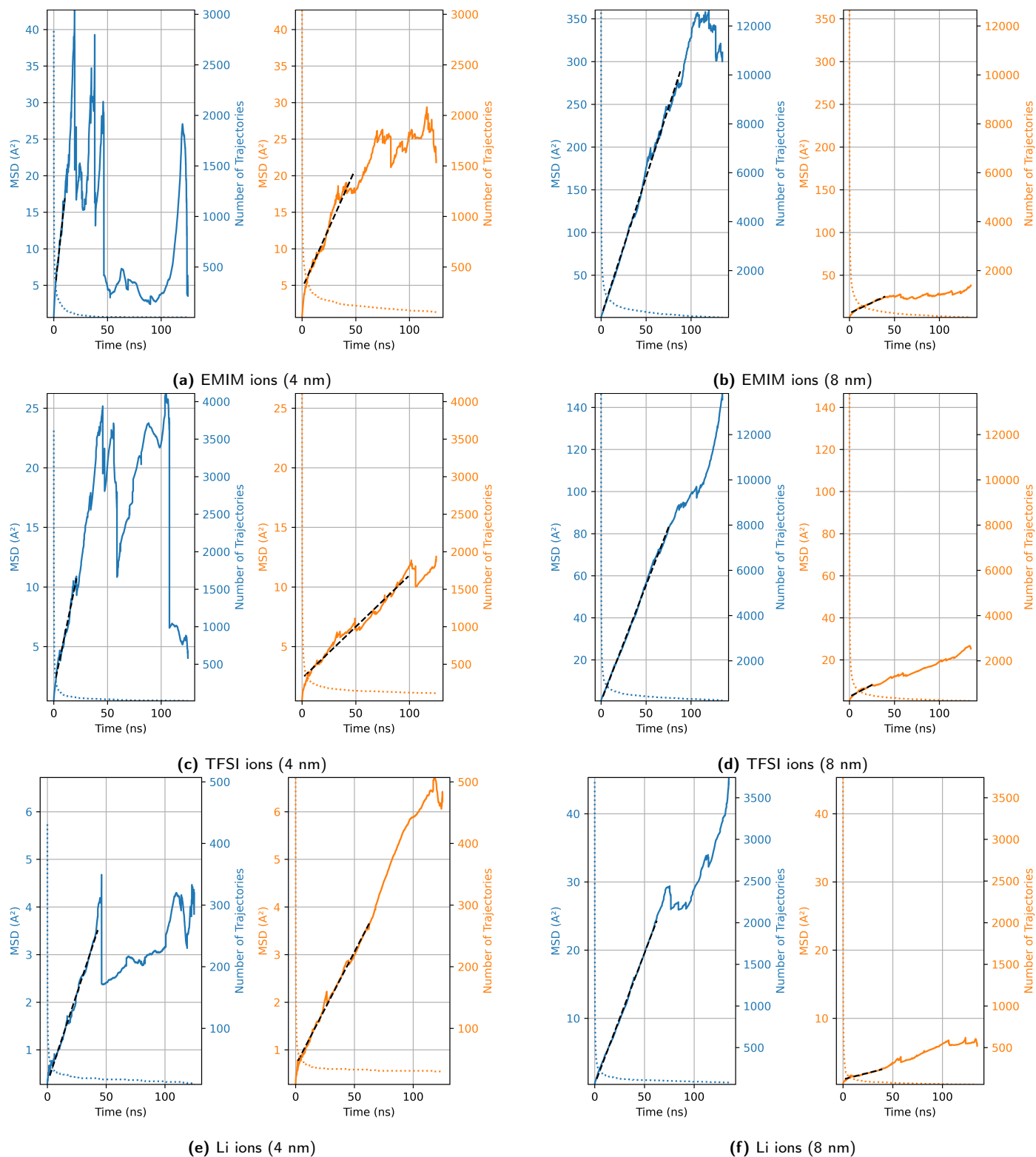


Figure S7 Fitting of MSD curves for different ions in the 4 nm and 8 nm confined [EMIM][TFSI] + Li(TFSI) systems across different spatial regions. The right axis corresponds to the number of individual ion trajectories that contribute to MSD curves. The black lines denote the fits to the curves.

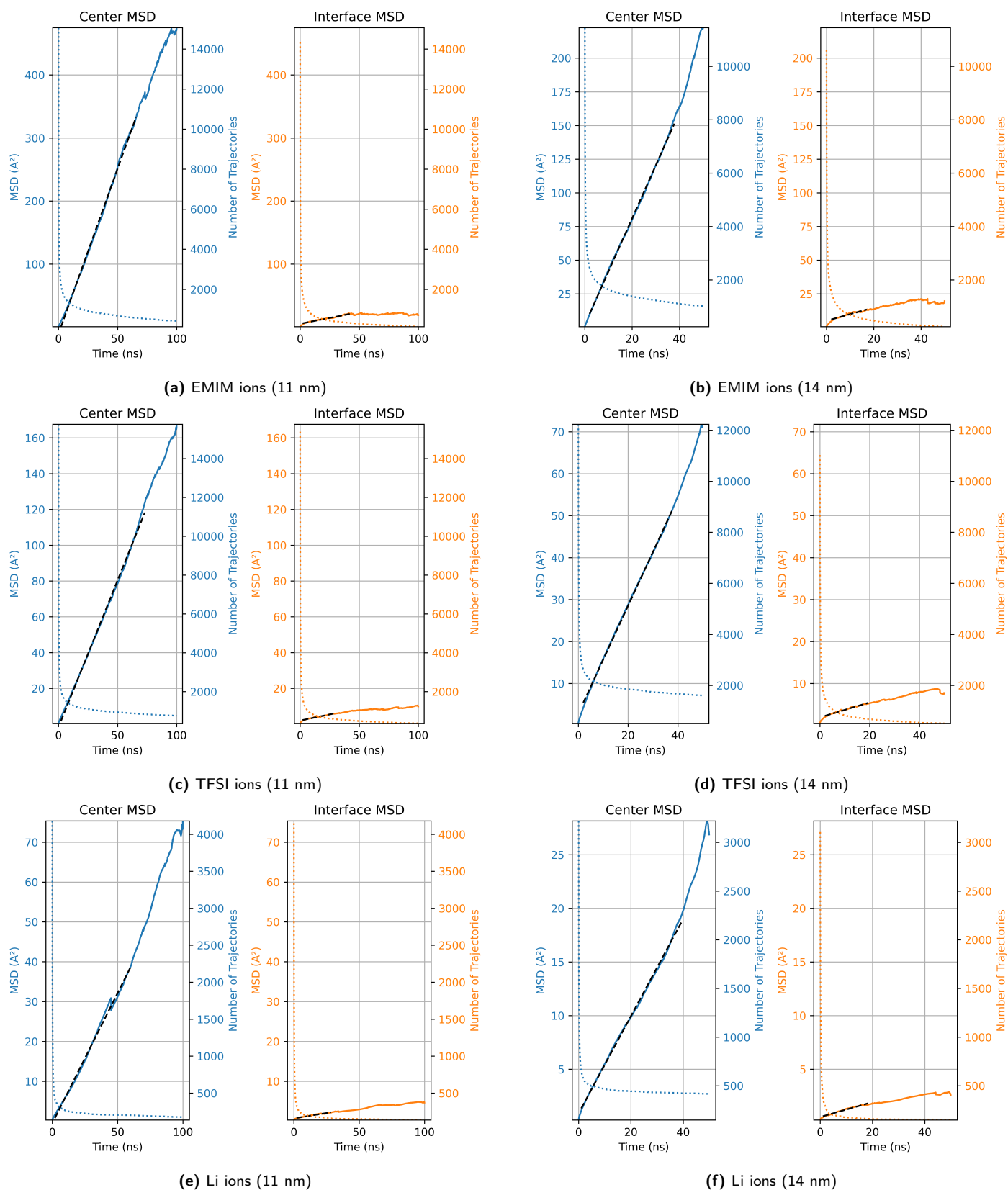


Figure S8 Fitting of MSD curves for different ions in the 11 nm and 14 nm confined [EMIM][TFSI] + Li(TFSI) systems across different spatial regions. The right axis corresponds to the number of individual trajectories of ions that contribute to MSD curves. The black lines denote the fits to the curves.

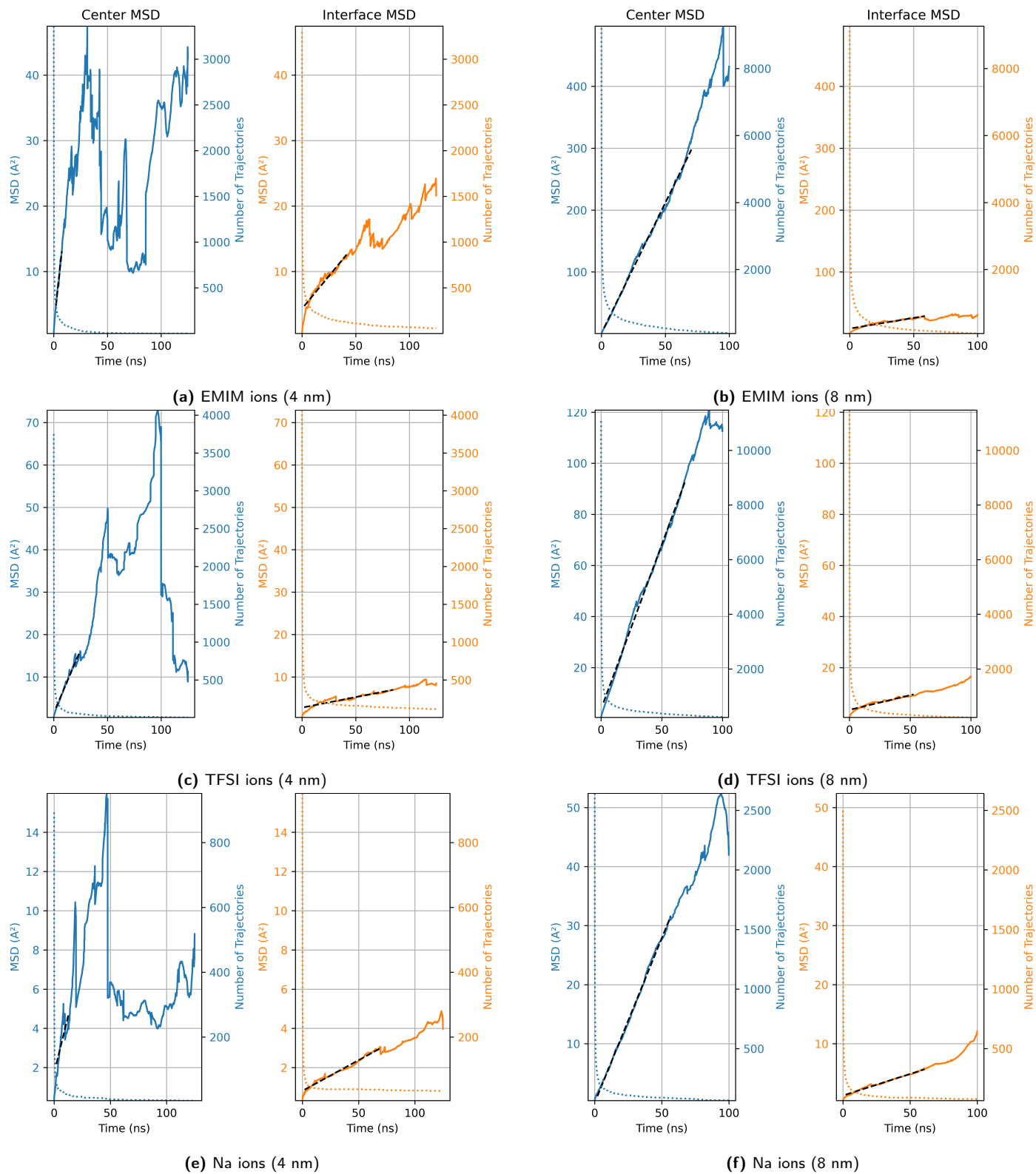


Figure S9 Fitting of MSD curves for different ions in the 4 nm and 8 nm confined [EMIM][TFSI] + Na(TFSI) systems across different spatial regions. The right axis corresponds to the number of individual trajectories of ions that contribute to MSD curves. The black lines denote the fits to the curves.

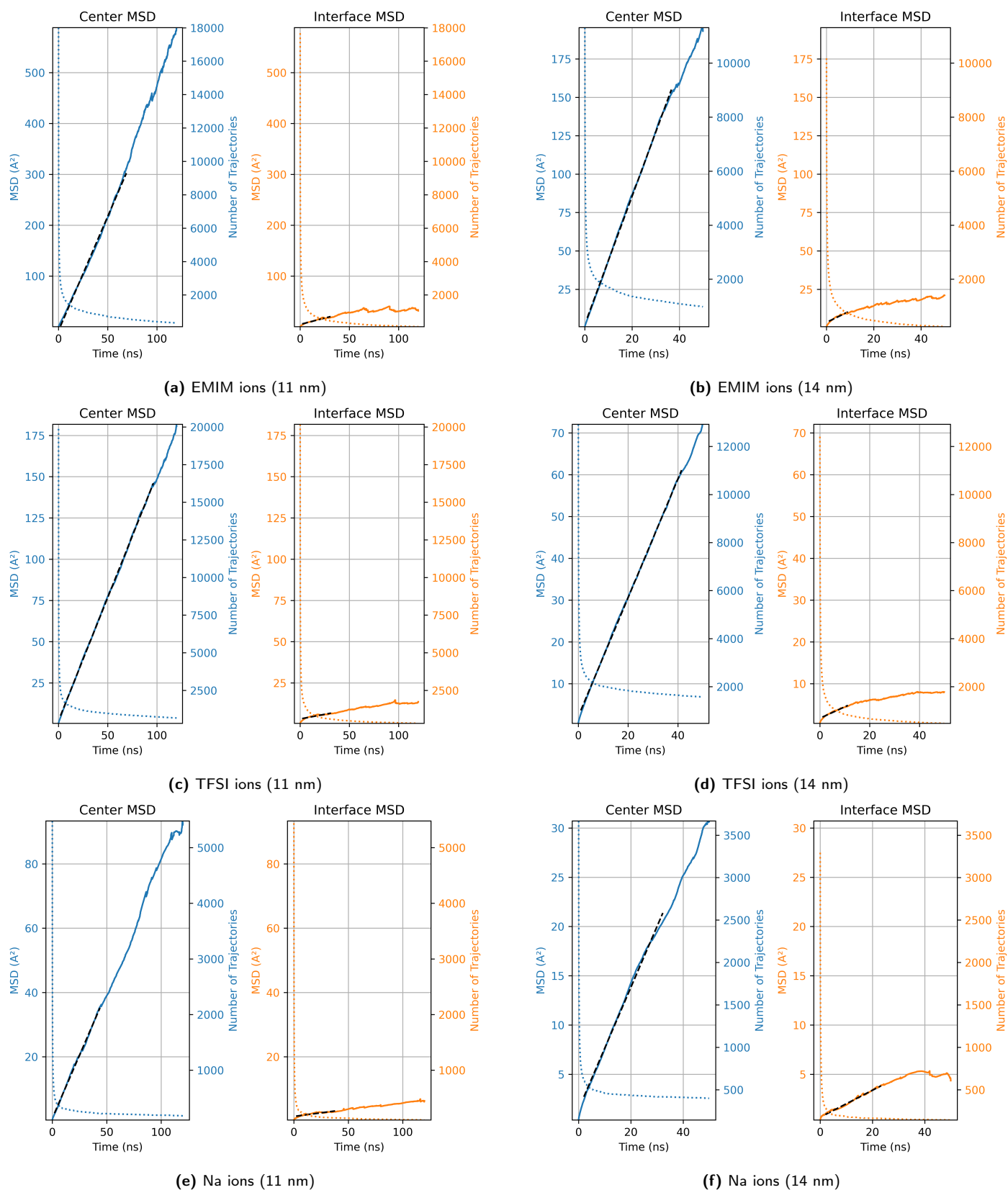


Figure S10 Fitting of MSD curves for different ions in the 11 nm and 14 nm confined [EMIM][TFSI] + Na(TFSI) systems across different spatial regions. The right axis corresponds to the number of individual trajectories of ions that contribute to MSD curves. The black lines denote the fits to the curves.

System	Diameter (nm)	Center			Interface		
		W_1	W_2	W_3	W_1	W_2	W_3
Li	4	7.02483×10^{-8}	9.68878×10^{-8}	7.68986×10^{-8}	9.69830×10^{-9}	1.95644×10^{-8}	1.986345×10^{-8}
	8	1.50494×10^{-7}	1.57564×10^{-7}	1.53816×10^{-7}	2.45411×10^{-8}	3.87313×10^{-8}	2.31181×10^{-8}
	11	2.10507×10^{-7}	2.28237×10^{-7}	2.61889×10^{-7}	5.26382×10^{-8}	5.26382×10^{-8}	1.85568×10^{-8}
	14	2.21451×10^{-7}	2.08200×10^{-7}	2.06963×10^{-7}	1.05308×10^{-7}	9.12150×10^{-8}	3.15830×10^{-8}
Na	4	8.30024×10^{-8}	1.16593×10^{-7}	8.85962×10^{-8}	1.31322×10^{-8}	1.46195×10^{-8}	1.59950×10^{-8}
	8	1.77813×10^{-7}	2.12170×10^{-7}	2.10045×10^{-7}	2.49263×10^{-8}	4.58494×10^{-8}	1.74528×10^{-8}
	11	1.86959×10^{-7}	2.02104×10^{-7}	2.18078×10^{-7}	2.40186×10^{-8}	4.53091×10^{-8}	2.33670×10^{-8}
	14	1.96260×10^{-7}	2.13345×10^{-7}	2.08788×10^{-7}	5.03180×10^{-8}	9.21243×10^{-8}	3.73927×10^{-8}

W_1 = Interface width 1 layer, W_2 = Interface width 2 layers, W_3 = Interface width 11 Å

Table S6 Region-wise diffusion coefficients with variable interface region widths for EMIM ions.

System	Diameter (nm)	Center			Interface		
		W_1	W_2	W_3	W_1	W_2	W_3
Li	4	2.69642×10^{-8}	4.47877×10^{-8}	2.84215×10^{-8}	7.10179×10^{-9}	6.62920×10^{-9}	4.51997×10^{-9}
	8	4.42558×10^{-8}	5.36547×10^{-8}	5.71315×10^{-8}	1.31463×10^{-8}	1.72517×10^{-8}	1.00078×10^{-8}
	11	6.29144×10^{-8}	7.24279×10^{-8}	8.20475×10^{-8}	1.63479×10^{-8}	2.11155×10^{-8}	6.87237×10^{-9}
	14	7.95144×10^{-8}	7.83112×10^{-8}	6.56179×10^{-8}	4.14818×10^{-8}	3.68452×10^{-8}	8.01188×10^{-9}
Na	4	2.72113×10^{-8}	4.70294×10^{-8}	2.95834×10^{-8}	6.12449×10^{-9}	5.04601×10^{-9}	2.98202×10^{-9}
	8	5.73405×10^{-8}	7.27976×10^{-8}	6.07490×10^{-8}	1.32901×10^{-8}	2.19965×10^{-8}	5.42989×10^{-9}
	11	6.50036×10^{-8}	7.75454×10^{-8}	7.29157×10^{-8}	1.57081×10^{-8}	2.39392×10^{-8}	5.07516×10^{-9}
	14	6.56384×10^{-8}	8.02454×10^{-8}	7.09911×10^{-8}	4.43750×10^{-8}	4.18728×10^{-8}	1.36538×10^{-8}

W_1 = Interface width 1 layer, W_2 = Interface width 2 layers, W_3 = Interface width 11 Å

Table S7 Region-wise diffusion coefficients with variable interface region widths for TFSI ions.

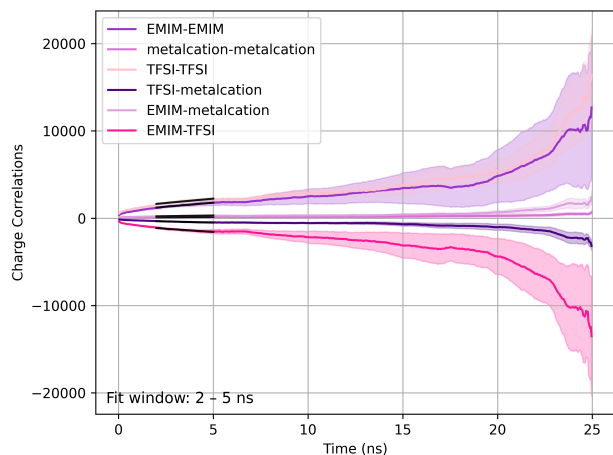
System	Diameter (nm)	Center			Interface		
		W_1	W_2	W_3	W_1	W_2	W_3
Li	4	5.93920×10^{-9}	6.10333×10^{-9}	7.65476×10^{-9}	2.49078×10^{-9}	3.93982×10^{-9}	2.35811×10^{-9}
	8	1.17876×10^{-8}	1.67957×10^{-8}	1.91755×10^{-8}	-	4.88755×10^{-9}	2.26549×10^{-9}
	11	2.51274×10^{-8}	3.10586×10^{-8}	3.26788×10^{-8}	1.30071×10^{-8}	7.13988×10^{-9}	2.67291×10^{-9}
	14	3.13843×10^{-8}	2.95791×10^{-8}	2.33594×10^{-8}	1.53170×10^{-8}	1.32232×10^{-8}	3.54112×10^{-9}
Na	4	5.99976×10^{-9}	1.42238×10^{-8}	7.65170×10^{-9}	4.84117×10^{-9}	3.98431×10^{-9}	2.65131×10^{-9}
	8	1.72920×10^{-8}	2.42663×10^{-8}	2.51635×10^{-8}	5.57159×10^{-9}	9.25507×10^{-9}	4.69539×10^{-9}
	11	2.73383×10^{-8}	3.70164×10^{-8}	3.86489×10^{-8}	2.06250×10^{-8}	1.04286×10^{-8}	2.49124×10^{-9}
	14	3.27094×10^{-8}	3.25382×10^{-8}	3.08937×10^{-8}	-	-	6.85320×10^{-9}

W_1 = Interface width 1 layer, W_2 = Interface width 2 layers, W_3 = Interface width 11 Å

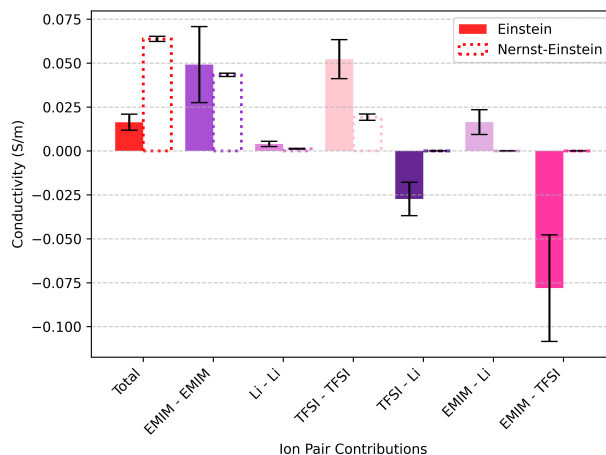
Table S8 Region-wise diffusion coefficients with variable interface region widths for metal cations.

8 Conductivity

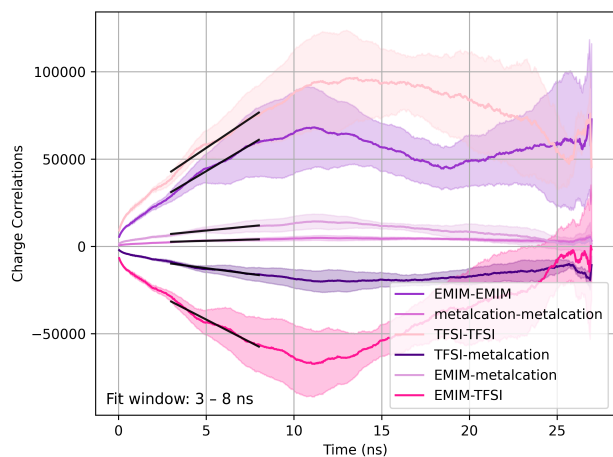
The conductivity bar plots for 0.24 concentration systems for all pore diameters are shown on the right side. The Einstein charge correlation graphs are shown on the left side along with the fit in the linear regime. However, care must be taken regarding the convergence of the curves at longer time scales. The shaded region in all the curves correspond to the confidence interval obtained by block averaging method.



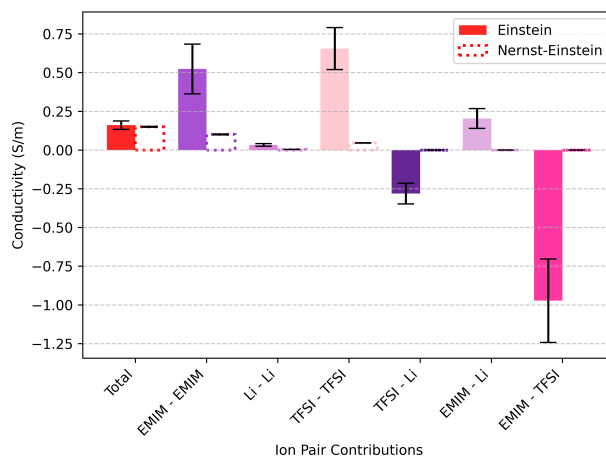
(a) Einstein charge correlations (Li, 4nm)



(b) Conductivity bar plot (Li, 4nm)

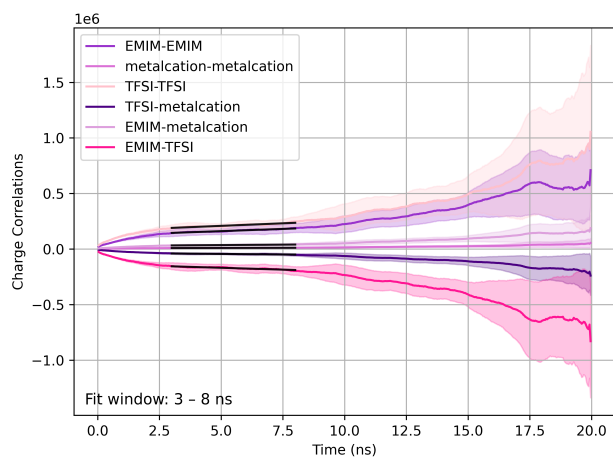


(c) Einstein charge correlations (Li, 8nm)

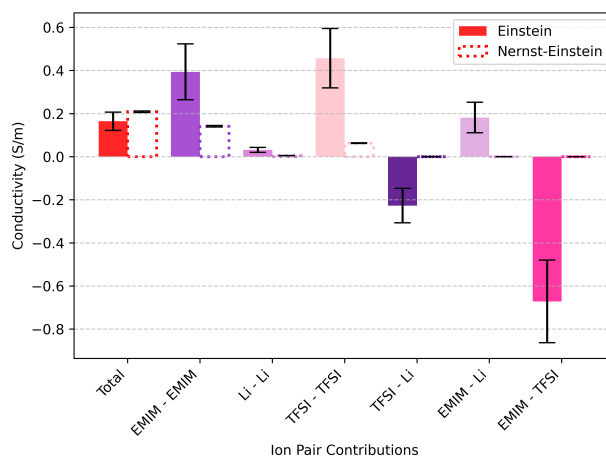


(d) Conductivity bar plot (Li, 8nm)

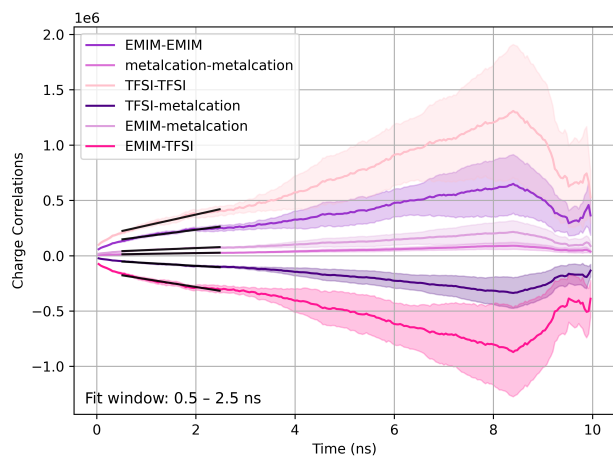
Figure S11 Einstein charge correlations and conductivity bar plots for Li^+ systems at 4 and 8 nm.



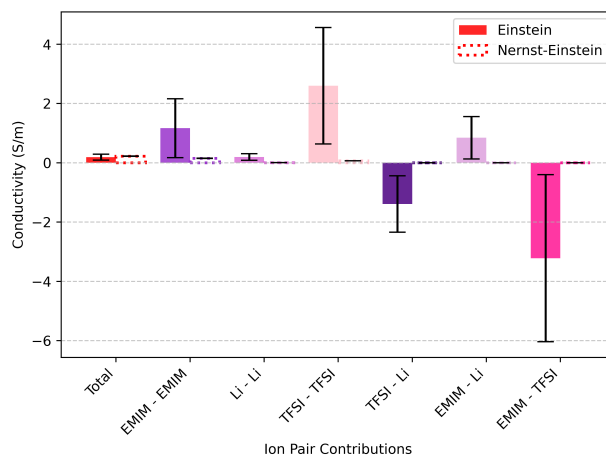
(a) Einstein charge correlations (Li, 11nm)



(b) Conductivity bar plot (Li, 11nm)

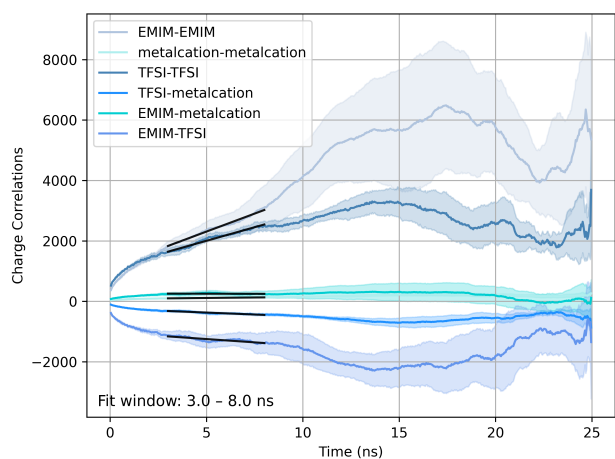


(c) Einstein charge correlations (Li, 14nm)

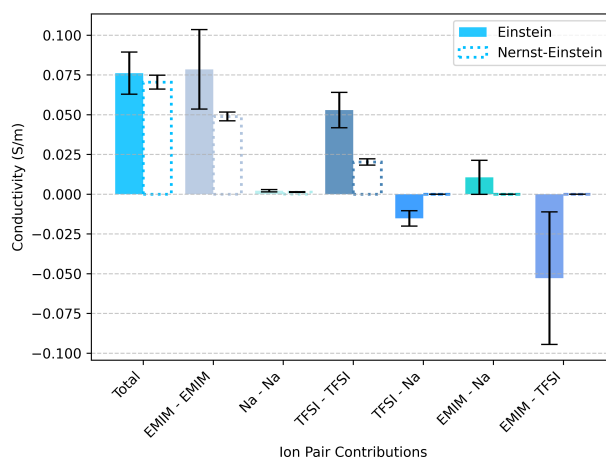


(d) Conductivity bar plot (Li, 14nm)

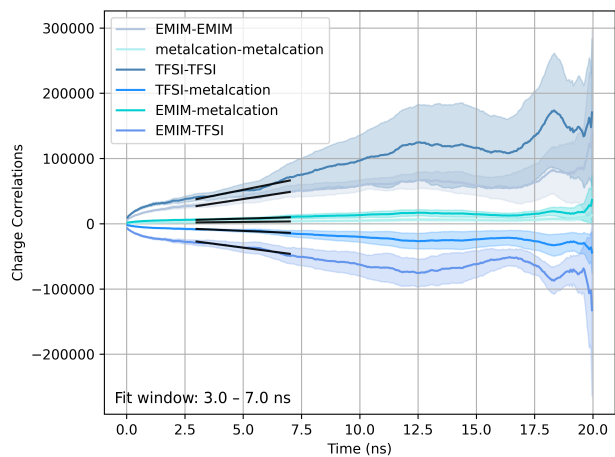
Figure S12 Einstein charge correlations and conductivity bar plots for Li^+ systems at 11 and 14 nm.



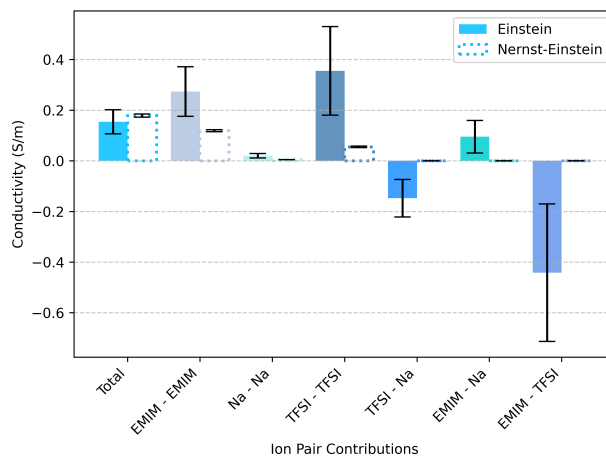
(a) Einstein charge correlations (Na, 4nm)



(b) Conductivity bar plot (Na, 4nm)

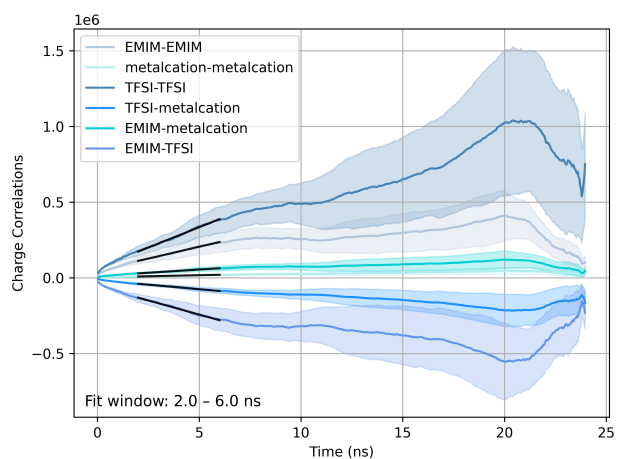


(c) Einstein charge correlations (Na, 8nm)

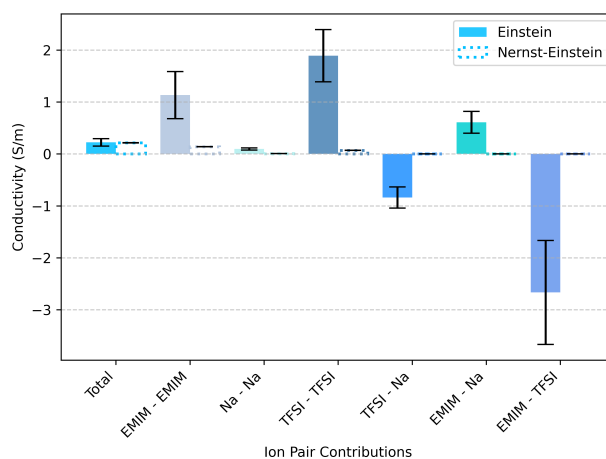


(d) Conductivity bar plot (Na, 8nm)

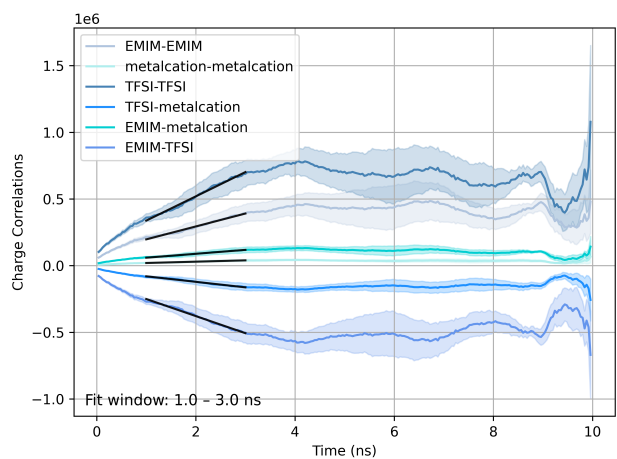
Figure S13 Einstein charge correlations and conductivity bar plots for Na⁺ systems at 4 and 8 nm.



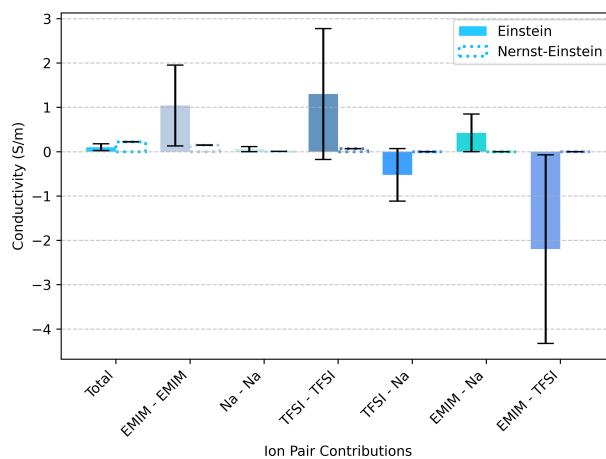
(a) Einstein charge correlations (Na, 11nm)



(b) Conductivity bar plot (Na, 11nm)



(c) Einstein charge correlations (Na, 14nm)



(d) Conductivity bar plot (Na, 14nm)

Figure S14 Einstein charge correlations and conductivity bar plots for Na^+ systems at 11 and 14 nm.

9 Check for charge drift along the pore axis

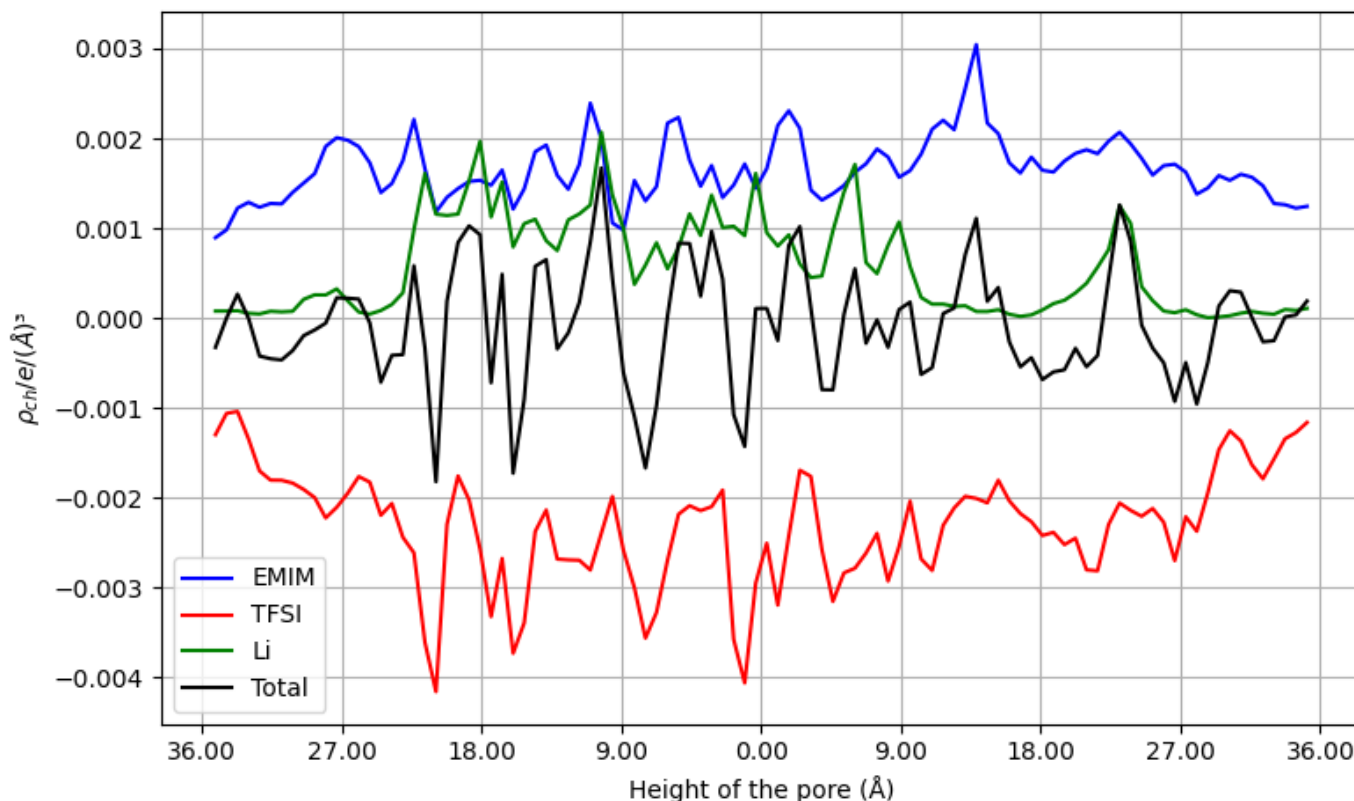


Figure S15 Axial charge density profile of ions of Li^+ system (0.24 mole fraction concentration) confined in 4 nm pore with height of 7.26 nm. The black line denotes the total charge density plotted as the sum of charge of all the ions. This check confirms no charge drift along the axis.

10 Simulation parameters

Thermostat damping parameter (T_{damp})	100 fs
Long-range solver (PPPM) accuracy	1e-5
LJ cut-off	12Å
Tail corrections	Not applied

Notes and references

- [1] H. Tokuda, K. Hayamizu, K. Ishii, M. A. B. H. Susan and M. Watanabe, *The Journal of Physical Chemistry B*, 2005, **109**, 6103–6110.
- [2] J. Gäding, G. Tocci, M. Busch, P. Huber and R. H. Meißner, *The Journal of Chemical Physics*, 2022, **156**, 064703.
- [3] S. Kunigal Vijaya Shankar, C. P. Ewels and Y. Claveau, *Journal of Chemical Information and Modeling*, 2026, **66**, 1617–1625.